Design of polarization-independent reflective metalens in near infrared waveband

Zhang Yuhui[1], Yang Bowei[1], Li Yiting[1], Zhao Yuanzhi[1], Fu Yuegang[1,2,3*]

(1. School of Optoelectric Engineering, Changchun University of Science and Technology, Changchun 130022, China;
2. Key Laboratory of Optoelectronic Measurement and Optical Information Transmission Technology of Ministry of Education, Changchun University of Science and Technology, Changchun 130022, China;
3. Key Laboratory of Advanced Optical System Design and Manufacturing Technology of the Universities of Jilin Province, Changchun 130022, China)

Abstract: Metalens has received extensive concern in recent years. Design of a polarization-independent reflective metalens was proposed baesd on Au in infrared waveband. MgF_2 was chosen as the dielectric spacer of the metalens. All simulations were carried out by using the finite-difference time-domain(FDTD) software. Results show that the proposed metalens has the same effect on different polarized light and can work well in the range of 700 - 850 nm and one-focus works best in the range of 750 - 800 nm. When the incidence wavelength is chosen as 800 nm, the proposed metalens can also work well for one-focus and multi-focus. At that time, the focal length of one focus, dual focus and three focus are 9.6, 6.6 and 4.7 μm, respectively. Different focus requirements can be realized according to the characteristics of the metalens.

Key words: polarization-independent; metalens; one-focus; multi-focus

CLC number: O436.3 **Document code:** A **DOI:** 10.3788/IRLA20200048

近红外波段偏振无关型反射超透镜的设计

张玉慧[1]，杨博伟[1]，李轶庭[1]，赵元埴[1]，付跃刚[1,2,3*]

(1. 长春理工大学 光电工程学院，吉林 长春 130022 ；
2. 长春理工大学 光电测控与光信息传输技术教育部重点实验室，吉林 长春 130022;
3. 吉林省先进光学设计与制造高校重点实验室，吉林 长春 130022)

摘　要：近些年,超透镜受到了广泛关注。文中提出了一种基于金材料的近红外波段偏振无关型反射超透镜,该超透镜采用 MgF_2 材料作为电介质层,利用 FDTD 软件实现仿真设计。仿真结果表明:超透镜在不同偏振光入射的情况下具有相同的聚焦效果,入射波长在 700~850 nm 的范围内,具有较好的聚焦效果。入射波长在 750 ~800 nm 范围内单焦点聚焦效果最好。当入射波长为 800 nm,该超透镜可以分别实现单焦点和多焦点聚焦,其单焦点、双焦点和三个焦点的焦距分别为 9.6、6.6 和 4.7 μm。可以利用该超透镜的特点实现不同的聚焦要求。

关键词：偏振无关； 超透镜； 单焦点； 多焦点

收稿日期:2020−02−16; 修订日期:2020−04−01

作者简介:张玉慧 (1992−), 女, 博士生, 主要从事仿生光学及微纳结构设计方面的研究。Email: 1615008053@qq.com

通讯作者:付跃刚 (1972−), 男, 教授, 博士, 主要从事光学设计及仿生光学等方面的研究。Email: fuyg@cust.edu.cn

0 Introduction

Metamaterials have many unusual phenomena, including negative refractive index, giant chirality, and indefinite permittivity[1−4], which made them widely investigated in recent years. Metasurfaces, the two dimensional versions of metamaterials, have been demonstrated to be a novel approach to control electromagnetic wavefronts[5−6]. Since Capasso et al. first investigated beam steering in 2011[7], many kinds of structures have been reported on metasurfaces to achieve the functions of focusing lens[8−10] and anomalous reflection and refraction[11]. Among many kinds of metasurfaces, metalens can achieve the function of focusing and anomalous reflection by configuring different materials and shapes of units. Lots of models like nanoslit[12], nanohole[13−14], graphene ribbons[15−19] are introduced in metalens design, where 2π phase shift resulted by the designed antennas is needed in controlling the wavefront. Although much structures have been proposed in past reports, the function of metalens have not been fully investigated.

In this paper, we proposed a new model based on Au and MgF_2, which is independence of polarization[20−21]. x-polarized and y-polarized incidence are both have the same focusing effect. The proposed metalens can work well in the range of 700 - 850 nm for one-focus, and by configuring the resonance antenna, the proposed metalens can also achieves dual focus and three focus. When we use the incidence of 800 nm wavelength, the focal length of one focus, dual focus and three focus are 9.6, 6.6 and 4.7 μm, respectively. The focal length will decrease as the focus number increases. We believe that our findings are beneficial in designing new function controlling devices.

1 Structure design

Figure 1 illustrates the schematic of the proposed lens, which is a metal-insulator-metal structure to form a Fabry-Perot cavity to enhance the interaction between light and resonance antenna. The resonance antenna and the bottom mirror are selected as Au with data acquired from reference [22]. The dielectric spacer is chosen as MgF_2 with a refrative index of 1.892[23]. The thicknesses of Au antenna, MgF_2 spacer and Au mirror shown in Fig.1(b) are set as t_a=30 nm, t_d=50 nm and t_s=130 nm, respectively. The top view of the unit cell of the metalens is shown in Fig.1(c). The period in x- and y-directions are p_x=p_y=200 nm. The resonance antenna is a circle, which is independent of different polarized light. Thus, we can control the wavefront of the plane wave regardless of x-polarization or y-polarization incidences. The working mechanism of the proposed metalens is shown in Fig.1(a). For numerical analysis, all simulations are carried out by using the finite-difference time-domain (FDTD) software.

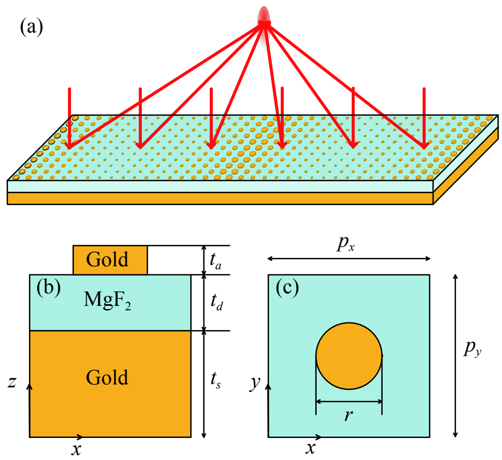

Fig.1 Schematic of proposed metalens. (a) Fragment; (b) Cross section view ; (c) Top view of proposed metalens

Generally, the resonant antenna is a circle, it has the same effect on different polarized light. To explore this, we choose the working wavelength as 800 nm. It shows the phase shift and reflectance of the reflected light for x-polarization incidence in Fig.2(a) and y-polarization incidence in Fig.2(b). A near 2π phase shift can be acquired when the radius r increases from 10 nm to 90 nm. As we can see, the change in the radius of the resonant antenna has the same effect on x-polarization incidence and y-polarization incidence.

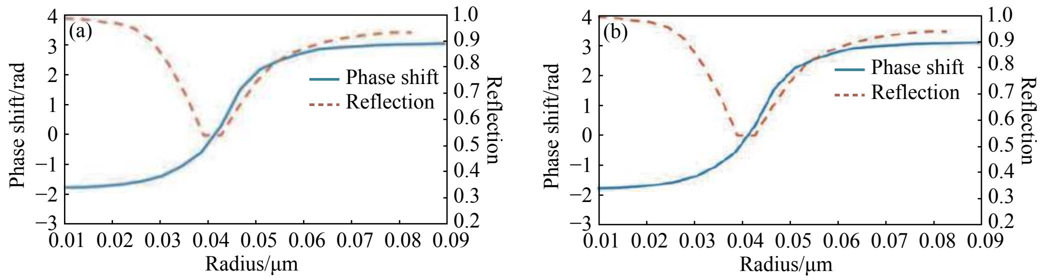

Fig.2 Phase shift and reflectance of reflected wave of (a) x-polarization incidence and (b) y-polarization incidence

2 Results and discussion

To design metalens to focus incident light, the phase profile of the metalens should follow the expression[24]:

$$\varphi(x)=\frac{2\pi}{\lambda_0}\left(\sqrt{x^2+F^2}-F\right) \tag{1}$$

where x is the horizontal position from the center of metalens; λ_0 is the wavelength of the incident; F is the focal length. Based on Eq.(1), we calculated the phase distribution curves for F=10 μm, and show them in Fig.3(a).

According to the expression, we selected the radius of the resonant antenna from Fig.2(a) and Fig.2(b) to design metalens. The focal length is designed as 10 μm

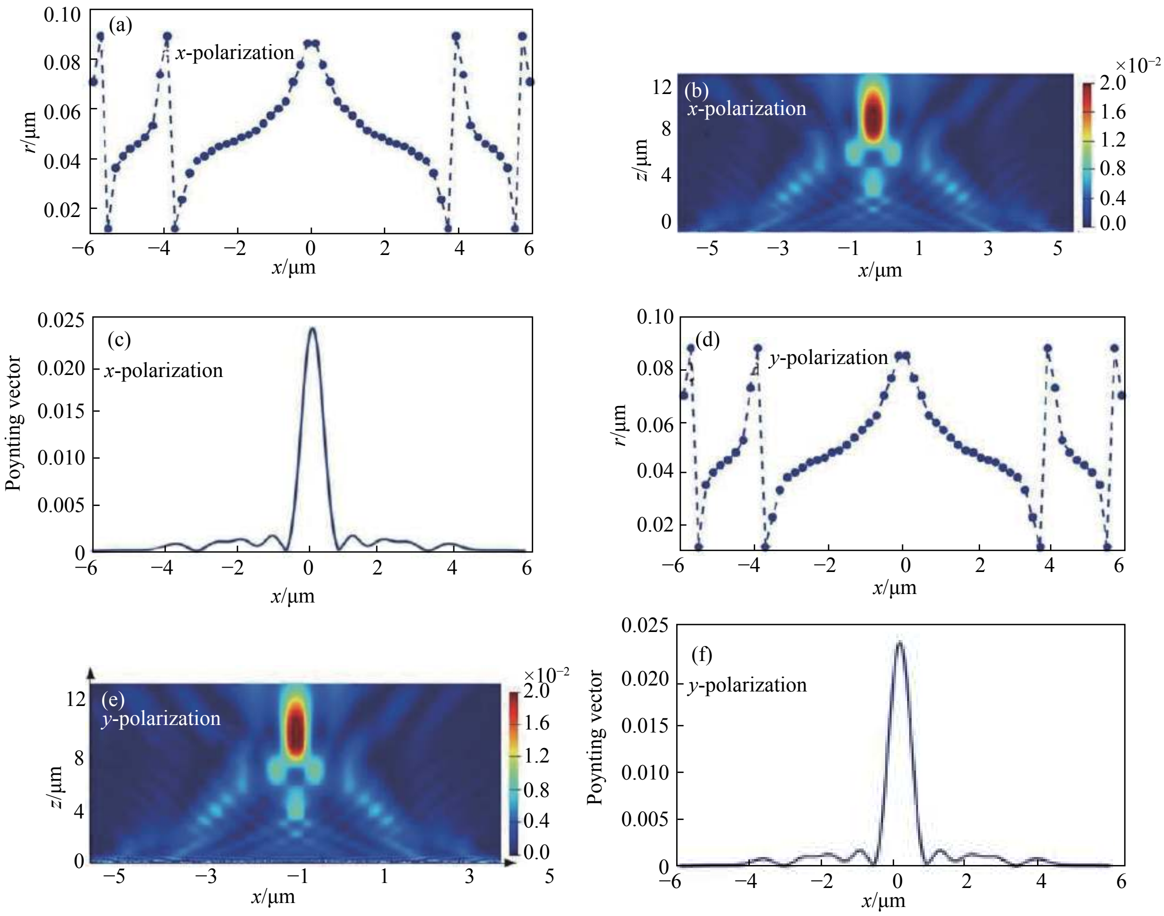

Fig.3 Proposed metalens working for one focus. (a) Relationship between the position x and radius of each unit for x-polarization; (b) Simulated Poynting vector distributions for metalens for x-polarization; (c) Intensities of the focusing spots along x direction for x-polarization; (d) Relationship between position x and the radius of each unit for y-polarization; (e) Simulated Poynting vector distributions for the metalens for y-polarization; (f) Intensities of the focusing spots along the x direction for y-polarization

and the size of the metalens is designed as 12 μm (60 units). The relationship between the position x and the radius of each unit for x-polarization and y-polarization are shown in Fig.3(a) and Fig.3(d) respectively. We simulated the metalens with 800 nm wavelength of the incident light. The Poynting vector distributions for incidence for x-polarization and y-polarization are shown in Fig.3(b) and Fig.3(e) respectively, (d) and the simulated focal lengths are both 9.6 μm, which agree well with the designed values. The intensity distributions along x-direction for x-polarization and y-polarization are shown in Fig.3(c) and Fig.3(f) respectively and the FWHM (Full Wave at Half Maximum) values for the focal lengths are both 0.67 μm. The results show that x-polarization and y-polarization have exactly the same focusing effect. The small deviations among the simulated focus length and the designed value are because the phase shift does not cover 2π, and we made the approximation when we selected the radius of the resonant antenna. On the other hand, the insufficient mesh accuracy may lead to deviations.

Then we simulated the proposed metalens in other incident wavelengths for x-polarization, thats 650, 700, 750, 850 and 900 nm. Simulated results are shown in Fig.4 and Fig.5. The poynting vector distributions for 650, 700, 750 , 850 and 900 nm are shown in Fig.4(a)−(e), respectively. The intensity distributions for 650, 700, 750, 850 and 900 nm along x-direction are shown in Fig.5(a)−(e), respectively. As we can see, the proposed metalens can works well within a broadband wavelength that ranges of 700−850 nm, and it performs best in the 750−800 nm range.

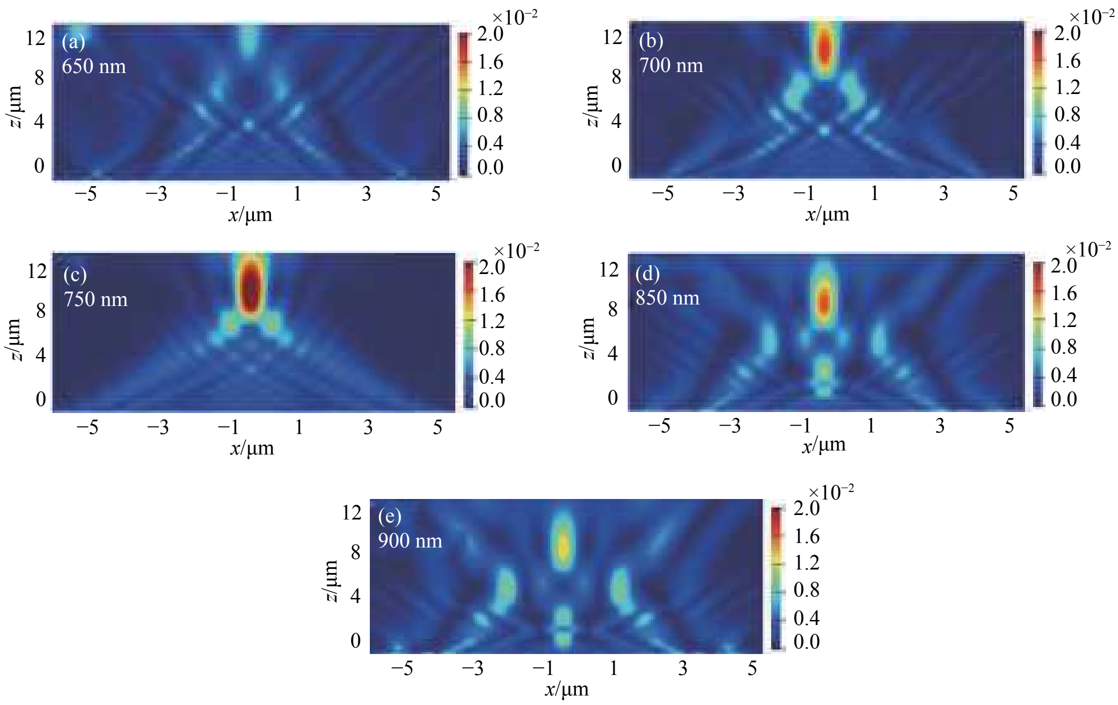

Fig.4 Simulated Poynting vector distributions for the metalens with incidence wavelength of (a) 650 nm, (b) 700 nm, (c) 750 nm, (d) 900 nm, (e) 850 nm

Further more, the proposed metalens can achieve dual focus by configuring the resonance antenna according to the expression:

$$a(x)\mathrm{e}^{-i\varphi(x)} = a_1\mathrm{e}^{-i\frac{2\pi}{\lambda}\left(\sqrt{(x-d/2)^2+f^2}-f\right)} + a_2\mathrm{e}^{-i\frac{2\pi}{\lambda}\left(\sqrt{(x+d/2)^2+f^2}-f\right)} \quad (2)$$

where $a(x)$ is the nearest amplitude, d is the distance between the two focals and a_1=a_2=0.5. We designed two focus locate at x=−3, x=3 and the focal lengths are both 10 μm. The relationship between the position x and the radius of each unit is shown in Fig.6(a). We simulated the

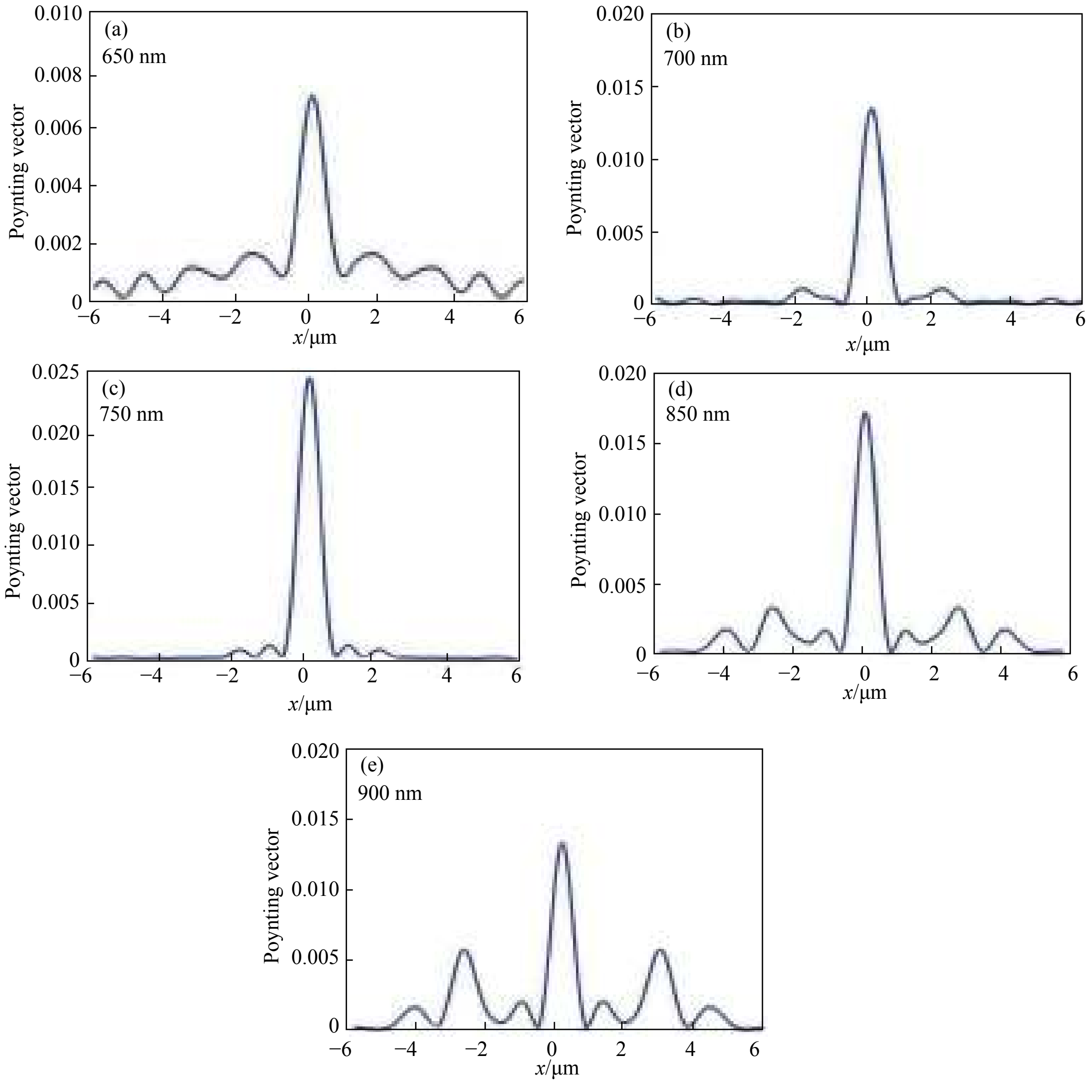

Fig.5 Intensities of the focusing spots along the x direction with the incidence wavelength of (a) 650 nm, (b) 700 nm, (c) 750 nm, (d) 850 nm, (e) 900 nm

metalens with 800 nm wavelength of the incident light. The Poynting vector distributions for incidence and the intensity distributions along x-direction are shown in Fig.6(b) and Fig.6(c), respectively. The simulated focal lengths are 6.6 μm and the FWHM values are 0.95 μm. The simulated results are in good agreement with the designed values. Note that there are small deviations among the simulated focus length and the designed value, which due to the approximations in selecting the radius of the resonant antenna in configuring processes and the insufficient mesh accuracy.

Then we designed three focus by the proposed metalens. According to the expression:

$$a(x)e^{-i\varphi(x)} = a_1 e^{-i\frac{2\pi}{\lambda}\left(\sqrt{(x-d/2)^2+f^2}-f\right)} + a_2 e^{-i\frac{2\pi}{\lambda}\left(\sqrt{(x+d/2)^2+f^2}-f\right)} + a_3 e^{-i\frac{2\pi}{\lambda}\left(\sqrt{x^2+f^2}-f\right)} \tag{3}$$

where the $a(x)$ is the nearest amplitude, $a_1=a_2=a_3=1/3$. The designed three focus locate at $x=-4$, $x=0$, $x=4$ and the focal lengths are all 10 μm. We selected the radius of the resonant antenna according to Fig.7(a), which are the relationship between the position x and the radius of each unit. The Poynting vector distributions for incidence and the intensity distributions along x-direction of the simulated results are shown in Fig.7(b)and Fig.7(c). The focal lengths of Fig.7(b)are 4.7 μm and the FWHM values of Fig.7(c) are 0.86 μm. As can be seen from Fig.6 and

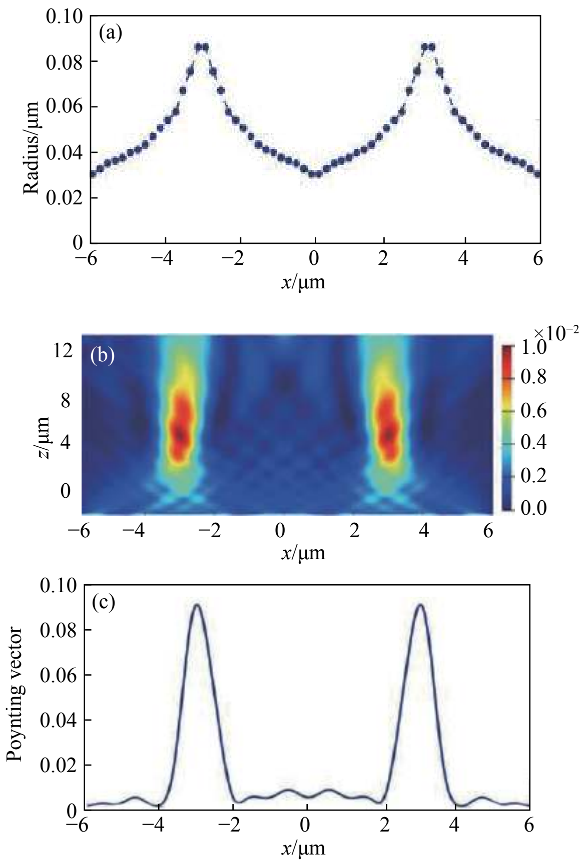

Fig.6 Proposed metalens working for daul focus. (a) Relationship between the position x and the radius of each unit; (b) Simulated Poynting vector distributions for the metalens; (c) Intensities of the focusing spots along the x direction

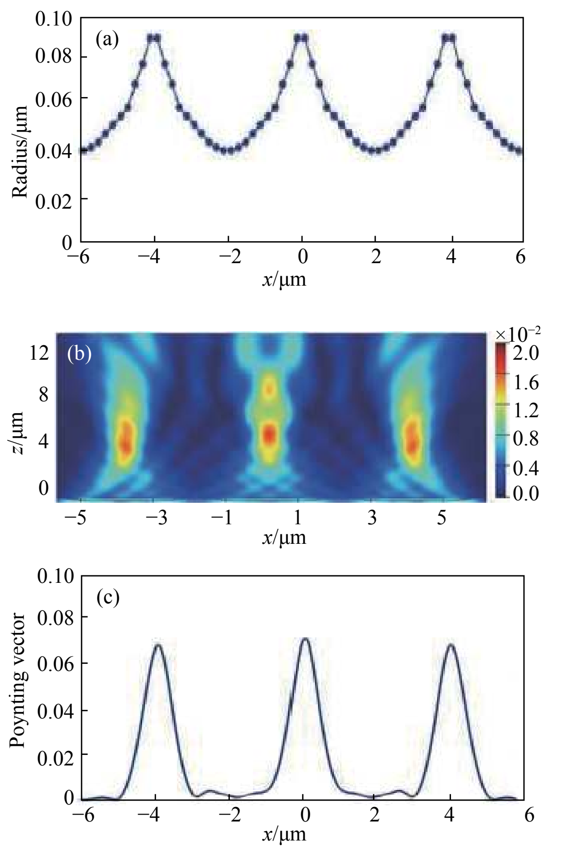

Fig.7 Proposed metalens working for three focus. (a) Relationship between the position x and the radius of each unit; (b) Simulated Poynting vector distributions for the metalens; (c) Intensities of the focusing spots along the x direction

Fig.7, the proposed structure also has a good focusing effect for multi-focus and the focal length will decrease as the focus number increases.

3 Conclusion

In summary, we proposed the metalens based on Au and MgF_2, which is independence of polarization. We simuated by using FDTD method. According to the simulated results, the proposed metalens can work well in the range of 700 nm to 850 nm and work best in the range of 750 nm to 800 nm for one focus. By configuring the resonance antenna, the proposed metalens can also work well for multi-focus. When the incidence wavelength is chosen as 800 nm, the focal length of one focus, dual focus and three focus are 9.6 μm, 6.6 μm and 4.7 μm, respectively. In conclusion, we can control the focus of the proposed metalens according to our requirements. We believe that our findings are beneficial in designing new function controlling devices.

References:

[1] Smith D R, Padilla W J, Vier D C, et al. Composite medium with simultaneously negative permeability and permittivity [J]. ***Phys Rev Lett***, 2000, 84(18): 4184−4187.

[2] Smith D R, Pendry J B, Wiltshire M C K . Metamaterials and negative refractive index [J]. ***Science***, 2004, 305(5685): 788−792.

[3] Zhou J F, Dong J F, Wang B N, et al. Negative refractive index due to chirality [J]. ***Phys Rev B***, 2009, 79(12): 121104.

[4] Chen H T, Taylor A J, Yu N. A review of metasurfaces: Physics and applications [J]. ***Rep Prog Phys***, 2016, 79(7): 1−41.

[5] Kildishev A V, Boltasseva A, Shalaev V M. Planar photonics with Metasurfaces [J]. ***Science***, 1232, 339(6125): 1232009.

[6] Lin D, Fan P, Hasman E,et al. Dielectric gradient metasurface optical elements [J]. ***Science***, 2014, 345(6194): 298−302.

[7] Yu N, Patrice G, Mikhail A, et al. Light propagation with phase discontinuities: Generalized laws of reflection and refraction [J]. ***Science***, 2011, 334(6054): 333−337.

[8] Li R, Guo Z, Wang W. Arbitrary focusing lens by holographic metasurface [J]. ***Photon Res***, 2015, 3(5): 252−255.

[9] Pors A, Nielsen M G, Eriksen R L, et al. Broadband focusing flat mirrors based on plasmonic gradient metasurfaces [J]. ***Nano Lett***, 2013, 13(2): 829−834.

[10] Lu D Y , Cao X , Wang K J, et al. Broadband reflective lens in visible bandbased on aluminum plasmonic metasurface [J]. ***Opt Exp***, 2018, 26(26): 34956−34964.

[11] Ni X, Emani N K, Kildishev A V, et al. Broadband light bending with plasmonic nanoantennas [J]. ***Science***, 2012, 335(6067): 427−427.

[12] Zhu Y, Yuan W, Li W, et al. TE-polarized design for metallic slit lenses: a way to deep-subwavelength focusing over a broad wavelength range [J]. ***Opt Lett***, 2018, 43(2): 206−209.

[13] Zhang J, Guo Z, Ge C, et al. Plasmonic focusing lens based on single-turn nano-pinholes array [J]. ***Opt Express***, 2015, 23(14): 17883−17891.

[14] Jia Y, Lan T, Liu P, et al. Polarization-insensitive, high numerical aperture metalens with nanoholes and surface corrugations [J]. ***Opt Commun***, 2018, 429: 100−105.

[15] Li Z, Yao K, Xia F, et al. Graphene plasmonic metasurfaces to steer infrared light [J]. ***Sci Rep***, 2015, 5: 1−9.

[16] Zhao H, Chen Z, Su F, et al. Terahertz wavefront manipulating by double-layer graphene ribbons metasurface [J]. ***Opt Commun***, 2017, 402: 523−526.

[17] Ma W, Huang Z, Bai X, et al. Dual-band light focusing using stacked graphene metasurfaces [J]. ***ACS Photonics***, 2017, 4(7): 1770−1775.

[18] Yao W, Tang L, Wang J, et al. Spectrally and spatially tunable terahertz metasurface lens based on graphene surface plasmons [J]. ***IEEE Photonics J***, 2018, 10(4): 1−8.

[19] Ma W, Huang Z, Bai X, et al. Tunable dual-band terahertz metalens based on stacked graphene metasurfaces [J]. ***Opt Commun***, 2018, 429(15): 41−45.

[20] Zhang X, Duan X, Muzychka Y, et al. High-efficiency metalenses with switchable functionalities in microwave region [J]. ***ACS Applied Materials & Interface***, 2019, 11(32): 28423−28430.

[21] Yuan Y, Zhang K, Ding X, et al. Complementary transmissive ultra-thin meta-deflectors for broadband polarization-independent refractions in the microwave region [J]. ***Photonics Research***, 2019, 7(1): 80−88.

[22] Johnson P B, Christy R W. Optical constants of the noble metals [J]. ***Phys Rev B***, 1972, 6(12): 4370.

[23] Sun S, Yang K, Wang C, et al. High-efficiency broadband anomalous reflection by gradient meta-surfaces [J]. ***Nano Lett***, 2012, 12(12): 6223−6229.

[24] Zhang Y, Zhao J, Zhou J, et al. Switchable polarization selective terahertz wavefront manipulation in a graphene metasurface [J]. ***IEEE Photonics J***, 2019, 11(3): 4600909.